FUDMA Journal of Sciences (FJS)
ISSN online: 2616-1370
ISSN print: 2645 - 2944
Vol. 7 No. 5, October, 2023, pp 54 - 63
DOI: https://doi.org/10.33003/fjs-2023-0705-1937

EQUILIBRIUM POINTS IN THE CR3BP OF THREE OBLATE BODIES UNDER THE EFFECTS OF CIRCUMBINARY DISC AND RADIATING PRIMARIES WITH POYNTING-ROBERTSON DRAG

[1]Udeme Monday Udo, [1]Aguda Ekele Vincent, *[2]Joel John Taura, [3]Tajudeen Oluwafemi Amuda

[1]Department of Mathematics, School of Basic Sciences, Nigeria Maritime University, Okerenkoko, Delta State, Nigeria
[2]Department of Mathematics and Computer Science, Federal University of Kashere, Gombe, Gombe State, Nigeria
[3]Department of Mathematics, Faculty of Sciences, Air Force Institute of Technology, Kaduna, Kaduna State, Nigeria

*Corresponding authors' email: taurajj@yahoo.com

ABSTRACT

We study numerically the generalized planar photogravitational circular restricted three-body problem, where an infinitesimal body is moving under the Newtonian gravitational attraction of two bodies which are finite, moving in circles around their center of mass fixed at the origin of the coordinate system, where both bodies are situated on the horizontal x-axis. The third body m is significantly smaller compared to the masses of the two bodies (primaries) where its influence on them can be neglected. The three participating bodies are modeled as oblate spheroids, under effect of radiation of the two main masses together with effective Poynting-Robertson drag and both of them are enclosed by a belt of homogeneous circular cluster of material points. In this paper, the existence and location of the equilibrium points and their linear stability are explored for various combinations of the model's parameters. We observe that under constant P–R drag effect, collinear equilibrium solutions cease to exist but there are in the absence of the drag forces. We found that five or seven non-collinear equilibrium points may lie on the plane of primaries motion depends on the particular values of model's parameters, and it is seen that the perturbing forces have significant effects on their positions and linear stability. In our model, the binary system Kruger 60 is used, and it is found that the positions of the equilibria and their stability are affected by these perturbing forces. In the case where seven critical points exist, all the equilibria are unstable except the equilibrium point (L_{n2}) which is always linearly stable while in the case where five critical points exist, all the points are unstable due to the presence of P–R drag effect.

Keywords: CR3BP, Radiation pressure, P-R drag, Oblateness, Equilibrium points, Stability

INTRODUCTION

The circular restricted three-body problem (CR3BP) studies the motion of a negligible mass moving in a system composed of two massive bodies (primaries) which move on circular orbits around their mutual centre of mass. The third body is significantly smaller compared to the masses of the two primaries where its influence on them can be neglected. The classics CR3BP admits five critical points; three of them, L_1, L_2, L_3 are on the x -axis and are called collinear, while the other two $L_4, L_5$are out of the x -axis and are called triangular (non-collinear) equilibrium points (EPs) of the problem. The three collinear points are generally unstable while the triangular points are generally stable for $0 < \mu < \mu_c \approx 0.03852090\ldots$ (Szebehely, 1967) where μ is the mass parameter and μ_c is the critical mass parameter. These equilibrium points are extensively used in space mission (see, e.g., Capdevila and Howell 2018 and references therein).

The classic R3BP considers the bodies involved to be spherical shapes; but in the solar (e.g., Sun, Earth, Jupiter and Saturn) and in the Stellar (e.g., Achernar, Alfa area, Kruger 60, Achird, Cen X-4) systems, some planets, stars and their satellites (Moon, Charon) are sufficiently oblate. The importance of considering non-spherical bodies in real systems in celestial mechanics was shown in Orberti and Vienne (2003), concluding that the addition of oblateness effects leads to significantly improved results regarding the approximation of real orbits of certain satellites in the solar system. This inspired several researchers (see e.g., Vincent et al. 2022, Vincent et al. 2024, Gyegwe et al. 2022; Kalantonis et al. 2008; Abouelmagd et al. 2013 and references therein) to include non-sphericity of the bodies in their studies of the CR3BP.

Stars (like our Sun) exert not only gravitation, but also radiation pressure on bodies moving nearby.

It was Poynting (1903) who first gave a description of the effect of radiation in the frame of relativity. Robertson (1937) took a cue from this to give an analysis of the effect of total radiation forces on a particle. Radzievskii (1950, 1953) studied what he named the photogravitational restricted three bodies problem, where the motion of an infinitesimal body is influenced by both the force of gravity and the radiation emitted from one of the primaries. Later on, many researchers have included radiation pressure force of either one or both primaries in the study of the CR3BP (Simmons et al. 1985; Schuerman 1980; Papadakis 1995, 1996, 2006; Papadakis et al. 2009; Gao and Wang 2020; Kalantonis et al. 2021; Stenborg 2008 among others). In estimating the light radiation force, all the above studies of photogravitational R3BPs have taken into account just one of the three components of the light pressure field, which is due to the central force: the gravitation and the radiation pressure. The other two components are arising from the Doppler shift and the absorption and subsequent re-emission of the incident radiation. These last two components constitute the so-called Poynting–Robertson (P–R) effect, which causes small particles of the solar system to spiral into the sun at a cosmically rapid rate. Knowing the importance of the P-R drag effect, many researchers like Stanley (1950), Chernikov (1970), Ragos and Zafiropoulos (1995), Lhotka and Celletti (2015), Singh and Amuda (2017), Pal and Kushvah (2015), Vincent and Perdiou (2021a, b), Vincent and Kalantonis (2023), Taura and Leke (2022), Tyokyaa and Atsue (2020), Vincent and Singh (2022) among others, devoted their work to study this problem with various characterizations. All these works have arrived at the conclusion that the P-R effect renders unstable those equilibrium points, which are conditionally stable in the classical case.

The discovery of numerous planetary systems has opened another avenue to understand the dynamics in both solar and planetary systems. Some planetary systems are found to have discs of dust or planetesimal or asteroids. These discs play important roles in the origin of planets' orbital elements if they are massive enough. The importance of the problem in astronomy has been addressed by Jiang and Yeh (2004, 2006) where it was shown that these perturbations exhibit significant changes in the number and equilibrium positions. Some researchers like Singh and Taura (2013), Kishor and Kushvah (2013), Vincent and Kalantonis (2023), Yousuf and Kishor (2019), Leke and Singh (2021), and others studied the R3BP by taking into account the gravitational potential from the belt under different characterizations.

In a recent study, Singh and Amuda (2017) have studied the locations and stability of the triangular EPs in the framework of the CR3BP when the primaries are radiating-oblate rigid bodies together with P-R drag from both massive bodies. They found that the positions of these points are affected from the radiation pressure, P–R drag and oblateness. They found that the EPs are unstable in the linear sense for the P–R effect against their conditional stability in the absence of the drag force. In the present work, we shall expand the investigation by considering the case where the two primaries are enclosed by cluster of material points together with an oblate infinitesimal body. As an application in this study, we consider the Kruger 60 binary system for which the positions and stability of the equilibrium points are calculated. The numerical methods for obtaining the positions of the EPs along with the linear stability follow the approach used in Vincent and Perdiou (2021a).

Equations of motion

We consider a barycentric coordinate system $Oxyz$ rotating relative to an inertial reference system with angular velocity ω about a common z −axis. Let the two massive bodies P_1 (bigger primary) and P_2 (smaller primary) have masses $m_1 = 1-\mu$ and$m_2 = \mu (0 < \mu \leq 1/2)$, respectively, with μbeing the mass-ratio parameter while the infinitesimal body is considered to have a mass m, which is significantly smaller than the masses of the primaries and therefore it does not affect their motion. We assume that the three bodies are oblate spheroids and the stars with their effective P-R drag are surrounded by a cluster of materials points. Following the works of Singh and Taura (2013) and Singh and Amuda (2017), the governing equations of motion of an infinitesimal mass under perturbing forces of radiation pressure, P-R drag and oblateness of the bodies coupled with the gravitational potential from cluster of materials around the primaries, have the form:

$$\ddot{x} - 2n\dot{y} = U_x - \frac{W_1}{r_1^2}\left[\frac{(x+\mu)}{r_1^2}\{(x+\mu)\dot{x} + y\dot{y}\} + \dot{x} - ny\right] - \frac{W_2}{r_2^2}\left[\frac{(x+\mu-1)}{r_2^2}\{(x+\mu-1)\dot{x} + y\dot{y}\} + \dot{x} - ny\right],$$

$$\ddot{y} + 2n\dot{x} = U_y - \frac{W_1}{r_1^2}\left[\frac{y}{r_1^2}\{(x+\mu)\dot{x} + y\dot{y}\} + \dot{y} + n(x+\mu)\right] - \frac{W_2}{r_2^2}\left[\frac{y}{r_2^2}\{(x+\mu-1)\dot{x} + y\dot{y}\} + \dot{y} + n(x+\mu-1)\right], \quad (1)$$

where

$$U_x = n^2 x - \frac{(1-\mu)(x+\mu)q_1}{r_1^3} - \frac{3(1-\mu)A_1(x+\mu)q_1}{2r_1^5} - \frac{\mu q_2(x+\mu-1)}{r_2^3} - \frac{3\mu(x+\mu-1)A_2 q_2}{2r_2^5} - \frac{3(1-\mu)(x+\mu)A_3}{2r_1^5} - \frac{3\mu(x+\mu-1)A_3}{2r_2^5} - \frac{M_b x}{(r^2+T^2)^{\frac{3}{2}}},$$

$$U_y = n^2 y - \frac{(1-\mu)yq_1}{r_1^3} - \frac{3(1-\mu)yq_1A_1}{2r_1^5} - \frac{\mu q_2 y}{r_2^3} - \frac{3\mu y A_2 q_2}{2r_2^5} - \frac{3(1-\mu)yA_3}{2r_1^5} - \frac{3\mu y A_3}{2r_2^5} - \frac{M_b y}{(r^2+T^2)^{\frac{3}{2}}}, \quad (2)$$

with

$$U = \frac{n^2}{2}(x^2+y^2) + \frac{(1-\mu)q_1}{r_1} + \frac{\mu q_2}{r_2} + \frac{(1-\mu)A_1 q_1}{2r_1^3} + \frac{\mu A_2 q_2}{2r_2^3} + \frac{(1-\mu)A_3}{2r_1^3} + \frac{\mu A_3}{2r_2^3} + \frac{M_b}{(r^2+T^2)^{\frac{1}{2}}},$$

$$r_1^2 = (x+\mu)^2 + y^2,\ r_2^2 = (x+\mu-1)^2 + y^2,\ W_1 = \frac{(1-\mu)(1-q_1)}{c_d},\ W_2 = \frac{\mu(1-q_2)}{c_d}, \quad (3)$$

$$n = \sqrt{1 + \frac{3}{2}(A_1+A_2) + \frac{2M_b r_c}{(r_c^2+T^2)^{\frac{3}{2}}}}.$$

Here $r_i (i = 1,2)$ are the distances of the third body from the bigger and smaller primaries, respectively, $q_1, q_2 (0 < q_i \leq 1, i = 1,2)$ and $W_1, W_2 (W_i << 1, i = 1,2)$ are the radiation pressure and P–R drag of the bigger and smaller primaries, respectively,$c_d$is the non-dimensional velocity of light while the dots denote differentiation with respect to time, t. Notice that when radiation force is absent, there will be no P–R drag force. $M_b (M_b << 1)$ is the total mass of the disc, $r$is the radial distance of the dust particle so that $r^2 = x^2 + y^2$while, $T = a + b$ defines the density profile of the accumulated materials with a and b being the flatness and core parameters, respectively, and n is the perturbed mean motion of the primaries. The oblateness of the three bodies come into the picture in the form of oblateness coefficients $0 \leq A_i = (A_{E_i}^2 - A_{P_i}^2)/5R^2 << 1, (i = 1,2,3)$ where A_{E_i} and A_{P_i} are the equatorial and polar radii of the bodies, respectively while$R$is the separation between the primaries.

Existence and positions of the equilibrium points

The necessary and sufficient conditions, which must satisfy for the existence of equilibrium points, are:$\ddot{x} = \ddot{y} = \dot{x} = \dot{y} = 0$. It thus follows from equations (1) and (2), that the equilibria are solutions of equations:

$$n^2x-\frac{(1-\mu)(x+\mu)q_1}{r_1^3}-\frac{3(1-\mu)A_1(x+\mu)q_1}{2r_1^5}-\frac{\mu q_2(x+\mu-1)}{r_2^3}-\frac{3\mu(x+\mu-1)A_2q_2}{2r_2^5}-\frac{3(1-\mu)(x+\mu)A_3}{2r_1^5}-\frac{3\mu(x+\mu-1)A_3}{2r_2^5}-\frac{M_bx}{(r^2+T^2)^{\frac{3}{2}}}+\frac{W_1ny}{r_1^2}+\frac{W_2ny}{r_2^2}=0, \quad (4)$$

and

$$n^2y-\frac{(1-\mu)yq_1}{r_1^3}-\frac{3(1-\mu)yq_1A_1}{2r_1^3}-\frac{\mu q_2y}{r_2^3}-\frac{3\mu yA_2q_2}{2r_2^5}-\frac{3(1-\mu)yA_3}{2r_1^5}-\frac{3\mu yA_3}{2r_2^5}-\frac{M_by}{(r^2+T^2)^{\frac{3}{2}}}-\frac{W_1n(x+y)}{r_1^2}-\frac{W_2n(x+\mu-1)}{r_2^2}=0 \quad (5)$$

The equations (4) and (5) lead to two types of solutions: the equilibria on the plane xy, i.e., the non-collinear points when $y\neq 0$and the collinear points when $y=0$.

Equilibrium points on the xaxis

The collinear (linear) equilibrium points are the ones lying on the x -axis of the synodic system. In the present problem, we observe that for $y=0$, the equation (5) is not satisfied due to the existence of the dissipative terms induced by the P-R drag force. This means that they exist no equilibrium solutions on the$x$ -axis in the present model's problem. This is no longer true when the drag forces are neglected. Therefore, we can conclude that under the constant effect of P-R drag, induced by the radiation pressure of the primaries, there are no equilibrium points that lie exactly on the x -axis, called collinear EPs. This agrees with the results of Ragos and Zafiropoulos (1995), Vincent et al. (2019) and others.

Equilibrium points on the (x,y) plane

The non-collinear equilibrium points are obtained by solving equations (4) and (5) simultaneously for $x\neq 0$ and$y\neq 0$. Note that, due to high complexity of the equations of motion there is an extra difficulty to solve both equations (4) and (5) analytically for all the EPs on the (x,y) plane which give the exact locations of the points of equilibrium (i.e. coordinates of the equilibrium points of the system) and to discuss the existence and the number of equilibria for every set of model's parameters. Consequently, we resort to numerical solutions of this model problem. This fact applies to similar studies, where numerical methods are used for determining the EPs of the system (see e.g., Ragos and Zafiropolous 1995; Vincent and Perdiou 2021a, b; Vincent and Kalantonis 2023). Figures 1—3 provide information regarding to different number of equilibria, for some assumed fixed values of the parameters. Specifically, in Figure 1 we illustrate the five equilibrium $L_i, i=1,2,\dots,5$ of the problem, for $q_1=0.985, q_2=0.999, C_d=299792458, \mu$ =0.255, $M_b=$ 0.05, $T=0.01$when the oblateness coefficients $A_1, A_2$and A_3vary: panels: (a) for $A_2=A_3=0$and $A_1=0.0015$, (b) $A_1=A_3=0$ and $A_2=0.0015$, (c) $A_1=A_2=0$and $A_3=0.0015$. We remark that for other values of these oblateness parameters, the number of non-collinear points remain same (collinear points cease to exist). We observe that the couple $L_{4,5}$are symmetric w.r.t the x -axis as well as that with the P-R drag effect, the existence of nonzero y components for L_1, L_2, L_3can be easily verified from equation (5), since the condition $y=0$is not satisfied for them.

In Figure 2, the positions of the five and seven non-collinear equilibrium points are illustrated for $q_1=0.985, q_2=0.999, A_1=0.0004, A_2=0.0003, A_3=0.0002, C_d=299792458$, and$T=0.01$when $\mu$and M_b vary. In particular, Figure 2a is when μ =0.255,M_b= 0.05, and in this case, there exist five non-collinear equilibrium points$L_i, i=1,2,\dots,5$, while Figure 2b is when μ =0.255 ,M_b= 0.09 , and in this case, there exist seven non-collinear equilibria, $L_i, i=1,2,\dots,5$and new additional equilibri aL_{n1},L_{n2} Finally, Figure 2c is when μ =0.385, $M_b=$ 0.05, and in this case the non-collinear equilibrium points are seven. We note here that the y -components of the equilibria L_1, L_2, L_3, L_{n1}, and L_{n2} are close to zero but not zero, which means that due to the$y$ -components these points are not collinear. From these results we can conclude that for some values of the system parameters, L_{n1} and L_{n2} do not in general exist even in the presence of the circular cluster of materials points, indicating that such equilibrium points only exist depend on the model's parameters. Further, it is noticed that the locations of all the EPs change with the primaries if the mass parameter changes.

In Figure 3, we illustrate the positions of the seven non-collinear EPs of the problem as well as the fixed location of the primaries as the radiation coefficient $q_1$varies (i.e., for $q_1=1, q_1=0.5$ and $q_1=0.3$ correspondingly) for fixed values of the parameters $\mu=0.255, q_2=0.999, A_1=0.0004, A_2=0.0003$, $A_3=0.0002, C_d=299792458, M_b=0.09$ and$T=0.01$. From Figure 3, we see that the equilibrium point L_2moves closer to the primary body $m_2$while all the EPs of the problem approach the primary body $m_1$as the radiation pressure of the bigger primary $q_1$tends to zero. We remark that the radiation pressure of the primary body $m_1$has the most effect on changing the equilibrium point locations.

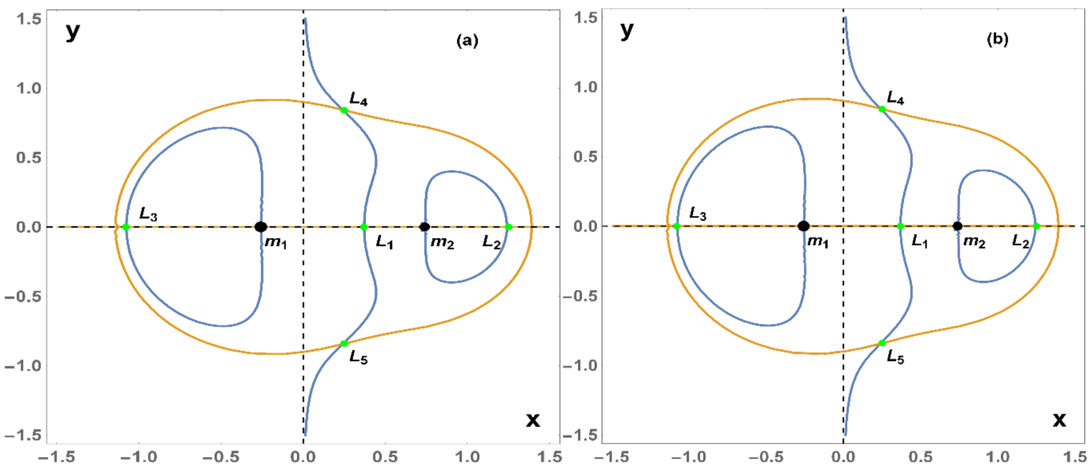

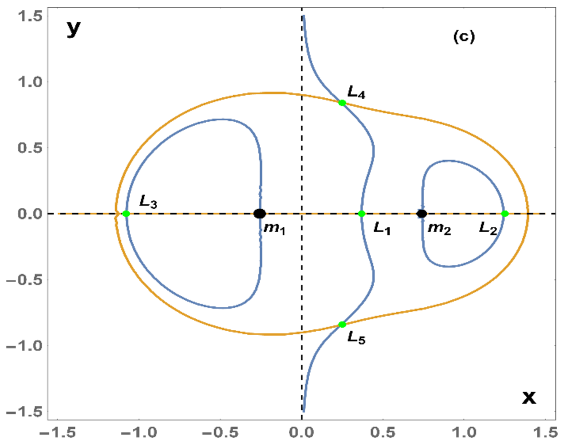

Figure 1: The positions of the five non-collinear equilibrium points $L_i, i = 1,2,\ldots,5$ (green dots) when $q_1 = 0.985, q_2 = 0.999, C_d = 299792458, \mu$ =0.255,M_b= 0.05, $T = 0.01$for different values of oblateness coefficients, i.e. panels: **(a)** for $A_2 = A_3 = 0$and $A_1 = 0.0015$, **(b)** $A_1 = A_3 = 0$ and $A_2 = 0.0015$, **(c)** $A_1 = A_2 = 0$and $A_3 = 0.0015$. Blue and brown curves correspond to the contour curves of equations (4) and (5), respectively, while the centers of the primary bodies, $m_i, i = 1,2$are denoted by black dots.

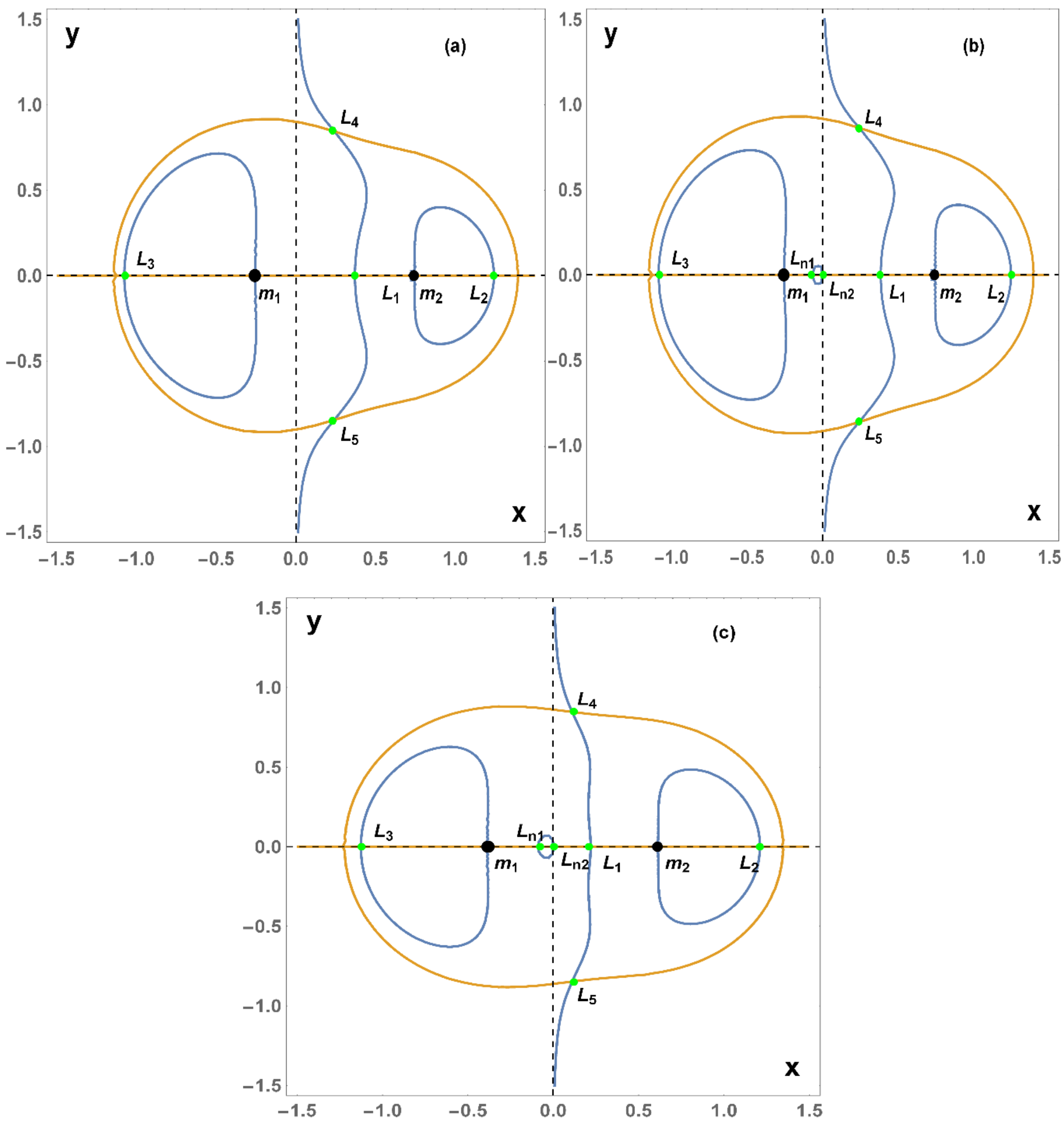

Figure 2: **(a)** Positions of the five non-collinear equilibrium points$L_i, i = 1,2,\ldots,5$for $\mu = 0.255, M_b = 0.05$, **(b)** Seven non-collinear equilibrium points $L_i, i = 1,2,\ldots,5, L_{n1}, L_{n2}$ for $\mu = 0.255, M_b = 0.09$, **(c)** Similar to panel **(b)**, but for $\mu = 0.385, M_b = 0.05$. The values of $q_1 = 0.985, q_2 = 0.999, A_1 = 0.0004, A_2 = 0.0003, A_3 = 0.0002, C_d = 299792458$, and$T = 0.01$are fixed in all cases.

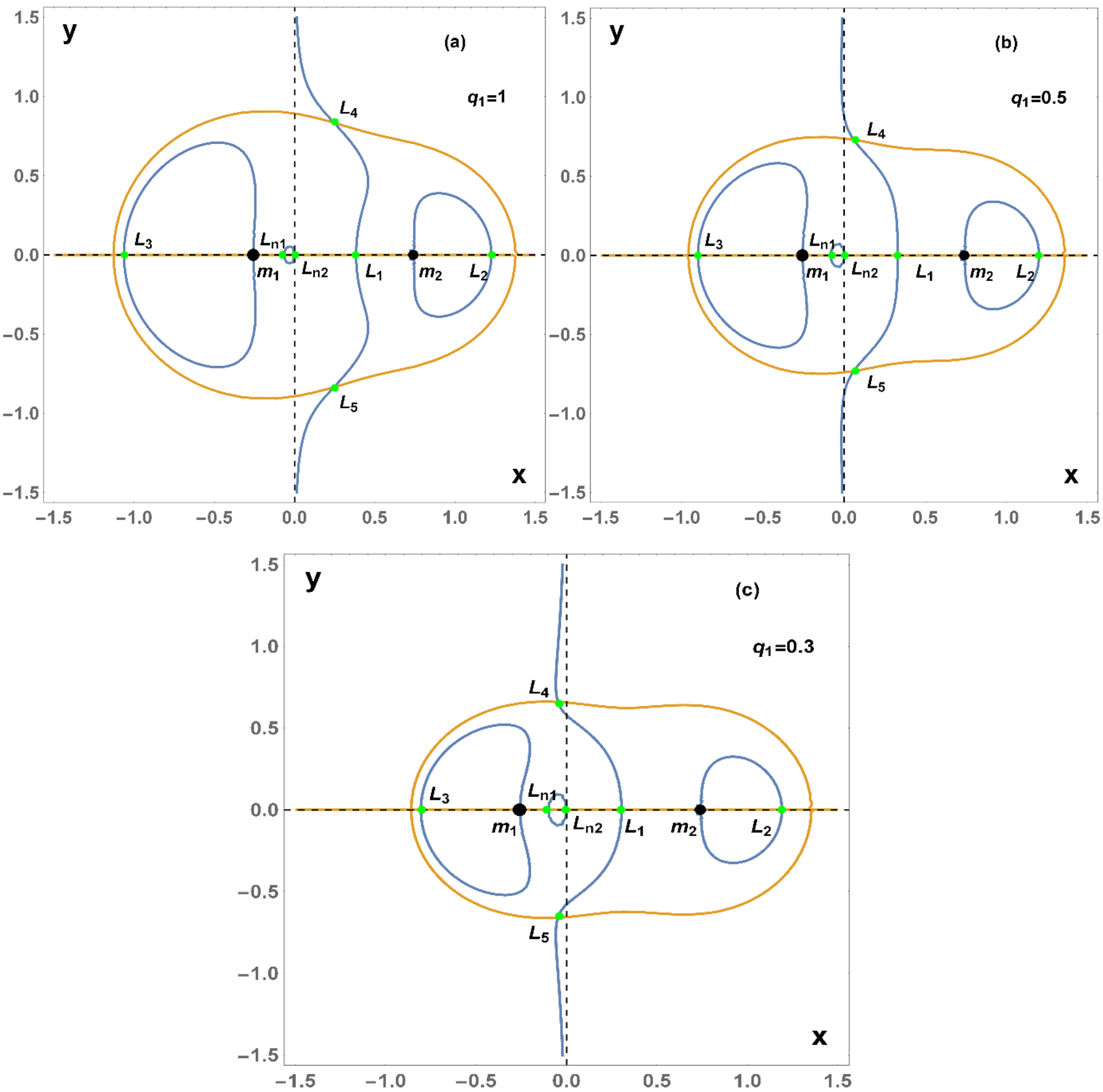

Figure 3: The position of the seven non-collinear equilibrium points $L_i, i = 1,2,\ldots,5, L_{n1}, L_{n2}$ for $\mu = 0.255, q_2 = 0.999, A_1 = 0.0004, A_2 = 0.0003, A_3 = 0.0002, C_d = 299792458, M_b = 0.09$ and $T = 0.01$ when only the radiation pressure of the bigger primary varies, i.e., panels: **(a)** for $q_1 = 1$, **(b)** $q_1 = 0.5$, and **(c)** $q_1 = 0.3$.

Linear stability of the non-collinear equilibrium points

Knowing the exact locations (x_0, y_0) of the equilibrium points, we can easily determine their linear stability or instability, through the nature of the roots of the characteristic equation. In doing this, we will follow the approach in Ragos and Zafiropoulos (1995) as well as Vincent and Perdiou (2021a, b). We suppose ξ and η are coordinates of the equilibrium point (x_0, y_0) such that

$$\xi = x - x_0, \eta = y - y_0 \tag{6}$$

Denoting the right-hand side of equation (1) by$\Omega_x = \frac{\partial \Omega}{\partial x}$and $\Omega_y = \frac{\partial \Omega}{\partial y}$, respectively, then the variational form of the equations of motion is derived as:

$$\begin{aligned} \ddot{\xi} - 2n\dot{\eta} &= \Omega_{x\dot{x}}^{(0)}\dot{\xi} + \Omega_{x\dot{y}}^{(0)}\dot{\eta} + \Omega_{xx}^{(0)}\xi + \Omega_{xy}^{(0)}\eta \\ \ddot{\eta} + 2n\dot{\xi} &= \Omega_{y\dot{x}}^{(0)}\dot{\xi} + \Omega_{y\dot{y}}^{(0)}\dot{\eta} + \Omega_{yx}^{(0)}\xi + \Omega_{yy}^{(0)}\eta \end{aligned} \tag{7}$$

where only the linear terms in ξ and η have been taken.

Then, the form of the characteristic polynomial corresponding to equations (7) is:

$$\lambda^4 + a_1\lambda^3 + a_2\lambda^2 + a_3\lambda + a_4 = 0, \tag{8}$$

with

$$a_1 = -(\Omega_{y\dot{y}}^{(0)} + \Omega_{x\dot{x}}^{(0)}), \quad a_2 = 4n^2 + \Omega_{x\dot{x}}^{(0)}\Omega_{y\dot{y}}^{(0)} - \Omega_{xx}^{(0)} - \Omega_{yy}^{(0)} - [\Omega_{x\dot{y}}^{(0)}]^2, \tag{9}$$

$$a_3 = \Omega_{x\dot{x}}^{(0)}\Omega_{yy}^{(0)} + \Omega_{xx}^{(0)}\Omega_{y\dot{y}}^{(0)} + 2n\Omega_{xy}^{(0)} - 2n\Omega_{yx}^{(0)} - \Omega_{y\dot{x}}^{(0)}\Omega_{xy}^{(0)} - \Omega_{yx}^{(0)}\Omega_{x\dot{y}}^{(0)}, \quad a_4 = \Omega_{xx}^{(0)}\Omega_{yy}^{(0)} - \Omega_{yx}^{(0)}\Omega_{xy}^{(0)}$$

The involved partial derivatives are given as:

$$\Omega_{xx}^{(0)} = n^2 - \frac{q_1(1-\mu)}{r_{10}^3} - \frac{q_2\mu}{r_{20}^3} + \frac{3q_1(1-\mu)(x_0+\mu)^2}{r_{10}^5} + \frac{3\mu q_2(x_0+\mu-1)^2}{r_{20}^5} - \frac{3A_1q_1(1-\mu)}{2r_{10}^5} - \frac{3A_2q_2\mu}{2r_{20}^5} - \frac{3A_3(1-\mu)}{2r_{10}^5} - \frac{3A_3\mu}{2r_{20}^5} + \frac{15A_1q_1(1-\mu)(x_0+\mu)^2}{2r_{10}^7} + \frac{15A_2q_2\mu(x_0+\mu-1)^2}{2r_{20}^7} + \frac{15A_3(1-\mu)(x_0+\mu)^2}{2r_{10}^7} + \frac{15A_3\mu(x_0+\mu-1)^2}{2r_{20}^7} - \frac{M_b}{(T^2+r_0^2)^{\frac{3}{2}}} + \frac{3M_bx_0^2}{(T^2+r_0^2)^{\frac{5}{2}}} - \frac{2nW_1y_0(x_0+\mu)}{r_{10}^4} - \frac{2nW_2y_0(x_0+\mu-1)}{r_{20}^4}, \tag{10}$$

$$\Omega_{yy}^{(0)} = n^2 - \frac{q_1(1-\mu)}{r_{10}^3} - \frac{q_2\mu}{r_{20}^3} + \frac{3q_1(1-\mu)y_0^2}{r_{10}^5} + \frac{3q_2\mu y_0^2}{r_{20}^5} - \frac{3A_1q_1(1-\mu)}{2r_{10}^5} - \frac{3A_2q_2\mu}{2r_{20}^5} - \frac{3A_3(1-\mu)}{2r_{10}^5} - \frac{3A_3\mu}{2r_{20}^5} + \frac{15A_1q_1(1-\mu)y_0^2}{2r_{10}^7} + \frac{15A_2q_2\mu y_0^2}{2r_{20}^7} + \frac{15A_3(1-\mu)y_0^2}{2r_{10}^7} + \frac{15A_3\mu y_0^2}{2r_{20}^7} - \frac{M_b}{(T^2+r^2)^{\frac{3}{2}}} + \frac{3M_by_0^2}{(T^2+r_0^2)^{\frac{5}{2}}} + \frac{2nW_1y_0(x_0+\mu)}{r_{10}^4} + \frac{2nW_2y_0(x_0+\mu-1)}{r_{20}^4}, \tag{11}$$

$$\Omega_{xy}^{(0)} = \frac{3q_1y_0(1-\mu)(x_0+\mu)}{r_{10}^5} + \frac{3q_2\mu y_0(x_0+\mu-1)}{r_{20}^5} + \frac{15A_1q_1y_0(1-\mu)(x_0+\mu)}{2r_{10}^7} + \frac{15A_2q_2\mu y_0(x_0+\mu-1)}{2r_{20}^7} + \frac{15A_3y_0(1-\mu)(x_0+\mu)}{2r_{10}^7} + \frac{15A_3\mu y_0(x_0+\mu-1)}{2r_{20}^7} + \frac{3M_bx_0y_0}{(T^2+r_0^2)^{\frac{5}{2}}} + \frac{nW_1}{r_{10}^2} + \frac{nW_2}{r_{20}^2} - \frac{2nW_1y_0^2}{r_{10}^4} - \frac{2nW_2y_0^2}{r_{20}^4}, \tag{12}$$

$$\Omega_{yx}^{(0)} = \frac{3q_1y_0(1-\mu)(x_0+\mu)}{r_{10}^5} + \frac{3q_2\mu y_0(x_0+\mu-1)}{r_{20}^5} + \frac{15A_1q_1y_0(1-\mu)(x_0+\mu)}{2r_{10}^7} + \frac{15A_2q_2\mu y_0(x_0+\mu-1)}{2r_{20}^7} + \frac{15A_3y_0(1-\mu)(x_0+\mu)}{2r_{10}^7} + \frac{15A_3\mu y_0(x_0+\mu-1)}{2r_{20}^7} + \frac{3M_bx_0y_0}{(T^2+r_0^2)^{\frac{5}{2}}} - \frac{nW_1}{r_{10}^2} - \frac{nW_2}{r_{20}^2} + \frac{2nW_1(x_0+\mu)^2}{r_{10}^4} + \frac{2nW_2(x_0+\mu-1)^2}{r_{20}^4}, \tag{13}$$

$$\Omega_{x\dot{x}}^{(0)} = -\frac{W_1}{r_{10}^2}\Big((1+\frac{x_0^2}{r_{10}^2}) + \frac{\mu}{r_{10}^2}(\mu+2x_0)\Big) - \frac{W_2}{r_{20}^2}\Big((1+\frac{1}{r_{20}^2}) - \frac{x_0}{r_{20}^2}(2-x_0) - \frac{\mu}{r_{20}^2}(2(1-x_0)-\mu)\Big), \tag{14}$$

$$\Omega_{y\dot{y}}^{(0)} = -\frac{W_1}{r_{10}^2}\Big(1+\frac{y_0^2}{r_{10}^2}\Big) - \frac{W_2}{r_{20}^2}\Big(1+\frac{y_0^2}{r_{20}^2}\Big), \tag{15}$$

$$\Omega_{x\dot{y}}^{(0)} = -\frac{W_1y_0}{r_{10}^4}(\mu+x_0) + \frac{W_2y_0}{r_{20}^4}(1-(x_0+\mu)) = \Omega_{y\dot{x}}^{(0)}, \quad 16)$$

where

$$r_{10}^2 = (x_0+\mu)^2 + {y_0}^2,\ r_{20}^2 = (x_0+\mu-1)^2 + {y_0}^2 \tag{17}$$

The determination of the stability or instability of motion around the non-collinear equilibrium points can be accomplished through the computation of the characteristic roots (i.e., equation (8)). An equilibrium point (x_0, y_0) will be stable if equation (8), evaluated at the equilibrium has four pure imaginary roots or four complex roots with each of them having negative real parts; otherwise, it is unstable.

Numerical Application: Kruger 60 binary system

We have computed and examined numerically as well as graphically the positions of the seven non-collinear equilibrium points and their stability for the binary system Kruger 60. In Table 1 are given (Singh and Amuda, 2017), the physical parameters of this binary system.

Table 1a. Numerical data for the binary Kruger 60 system (Singh and Amuda 2017)

Binary system	Mass ($M_\otimes$)		Luminosity (L_0)		Binary separation	Dimensionless speed of light	Mass ratio
	m_1	m_2	L_1	L_2	a	c_d	μ
Kruger 60	0.271	0.176	0.01	0.0034	9.5	46,393.84	0.3937

Table 1b. Numerical data for the binary Kruger 60 system (Singh and Amuda 2017)

Binary system	Radiation pressure (q_i)	
	q_1	q_2
Kruger 60	0.99992	0.99996

Firstly, the effect of mass of the disc (M_b) of both primaries on the positions of the non-collinear equilibria for the binary system is shown in Table 2 for fixed values of the remaining parameters. It is observed that with the increase of M_b from 0 to 0.09 for fixed $\mu = 0.3937, q_1 = 0.99992$, $q_2 = 0.99996\ A_1 = 0.024$, $A_2 = 0.02, A_3 = 0.015$, $c_d = 46{,}393.84$, and $T = 0.01$, x −coordinates of L_1 increase while at the same time the y −coordinates decrease; both the$x$and y -coordinates of L_2, L_3, L_{n2} (where exist) and L_4 (the situation is same at the symmetric point L_5) decrease while both the x and y -coordinates of L_{n1} (where exist) increase. The overall effect due to the mass of the disc (M_b) of both primaries is that $L_1, L_2, L_3, L_{n2}, L_{4,5}$move closer to the Ox −axis while L_{n1} move away from the Ox −axis. It is obvious, that the mass of disc of the primary bodies affects the positions of the equilibrium points significantly. It is intuitively noted that the variation (difference in the positions/coordinates) of the equilibria L_1, L_2, L_3, L_{n1} and $L_{4,5}$ is the biggest whereas $L_{n2}$is nearly zero (Table 2).

Next, we shall discuss the positions of the non-collinear equilibrium points of the test body for the binary system Kruger 60 when the oblateness coefficientsA_1, A_2andA_3vary in the interval $A_i \in [0, 0.08], i = 1,2,3$ for fixed numerical value of μ, q_1, q_2, M_b, and T.

To investigate the influence of the oblateness parameter of the bigger primary A_1 on the positions of the equilibria under consideration, the oblateness coefficient of the smaller primary is arbitrary set to be $A_2 = 0.02$ while that of the infinitesimal third body is set to be $A_3 = 0.01$. The coordinates of the numerically determined non-collinear equilibria are shown in Table 3 for various values of the oblateness coefficient A_1. We observe that with the increase of A_1 (0 to 0.08) for fixed $\mu = 0.3937$, $q_1 = 0.99992, q_2 =$

0.99996, $A_2 = 0.02, A_3 = 0.01$, $M_b = 0.1$, $T = 0.01$, and $c_d = 46{,}393.84$, the coordinates of the seven non-collinear equilibria increase or decrease. In particular, the x −coordinates of equilibrium points L_1, L_3, and L_4 (the situation is same at the symmetric point L_5) increase while at the same time the y −coordinates decrease; both the x and y coordinates of the points L_2 and L_{n1} decrease whereas both the x and y coordinates of the point L_{n2} increase.

Similarly, for fixed oblateness coefficients $A_1 = 0.03$ and $A_3 = 0.01$ the locations of the equilibrium points with respect to different values of oblateness coefficient A_2 are presented in Table 4. We observe that with the increase of A_2, both the x and y coordinates of the points L_1, L_3, and L_4 (the situation is same at the symmetric point L_5) decrease; both the x and y coordinates of the point L_{n1} increase; x coordinates of point L_2 increase while at the same time y coordinates decrease; x coordinates of the point L_{n2} decrease while the y coordinates increase. For the investigation of the influence of the oblate infinitesimal body parameter A_3 on the positions of the equilibrium points we set for the oblateness of the bigger and smaller primary the values $A_1 = 0.03$ and $A_2 = 0.02$, respectively. The coordinates of the corresponding equilibrium points are shown in Table 5 for increasing values of oblateness coefficient A_3. We observe that with the increase of A_3 from 0 to 0.08, both the x and y coordinates of L_1 and L_{n1} decrease; both the x and y coordinates of L_2 and L_{n2} increase; x coordinates of L_3 increase; the y coordinates decrease while at the same time x coordinates of L_4 (the situation is same at the symmetric point L_5) decrease with increase in the y coordinates.

Table 2. The exact positions (x_0, y_0) of the seven non-collinear equilibrium points for varying mass disc for the binary system Kruger 60 when $\mu = 0.3937$, $q_1 = 0.99992$, $q_2 = 0.99996$ $A_1 = 0.024$, $A_2 = 0.02$, $A_3 = 0.015$, $T = 0.01$, and $c_d = 46{,}393.84$

M_b	L_1	L_2	L_3
0	0.147054, -1.43186×10^{-10}	1.24360, -1.52545×10^{-9}	-1.16614, 3.54274×10^{-9}
0.01	0.162423, -1.04806×10^{-10}	1.23863, -1.50605×10^{-9}	-1.16089, 3.51196×10^{-9}
0.03	0.182581, -7.64634×10^{-11}	1.22918, -1.46952×10^{-9}	-1.15091, 3.45402×10^{-9}
0.06	0.202605, -5.86602×10^{-11}	1.21609, -1.41973×10^{-9}	-1.13709, 3.37511×10^{-9}
0.09	0.217116, -4.90411×10^{-11}	1.20414, -1.37505×10^{-9}	-1.12447, 3.30441×10^{-9}
M_b	L_{n1}	L_{n2}	$L_{4(5)}$
0	−	−	0.108117, ± 0.862323
0.01	−	−	0.108116, ± 0.858575
0.03	-0.061946, -1.92162×10^{-11}	-1.3902×10^{-4}, -7.47658×10^{-14}	0.108114, ± 0.851595
0.06	-0.080537, -2.18648×10^{-11}	-6.9446×10^{-5}, -3.86392×10^{-14}	0.108112, ± 0.842258
0.09	-0.092862, -2.31955×10^{-11}	-4.6285×10^{-5}, -2.65748×10^{-14}	0.108110, ± 0.834068

Table 3. The exact positions (x_0, y_0) of the seven noncollinear equilibrium points for varying oblateness of the bigger primary body for the binary Kruger 60 system when $\mu = 0.3937$, $q_1 = 0.99992$, $q_2 = 0.99996$, $A_2 = 0.02$, $A_3 = 0.01$, $M_b = 0.1$, $T = 0.01$, and $c_d = 46{,}393.84$

A_1	L_1	L_2	L_3
0	0.220325, -4.75935×10^{-11}	1.20279, -1.38564×10^{-9}	-1.10963, 3.36583×10^{-9}
0.02	0.222839, -4.73199×10^{-11}	1.19764, -1.36455×10^{-9}	-1.11622, 3.29800×10^{-9}
0.04	0.225272, -4.70085×10^{-11}	1.19266, -1.34432×10^{-9}	-1.12202, 3.23521×10^{-9}
0.06	0.227630, -4.66649×10^{-11}	1.18785, -1.32490×10^{-9}	-1.12718, 3.17668×10^{-9}
0.08	0.229914, -4.62938×10^{-11}	1.18318, -1.30623×10^{-9}	-1.13181, 3.12184×10^{-9}
A_1	L_{n1}	L_{n2}	$L_{4(5)}$
0	-0.10964, -3.43328×10^{-11}	-3.08874×10^{-5}, -2.3827×10^{-14}	0.096788, ± 0.833430
0.02	-0.09961, -2.60355×10^{-11}	-3.84633×10^{-5}, -2.4102×10^{-14}	0.106288, ± 0.829942
0.04	-0.09259, -2.11422×10^{-11}	-4.60406×10^{-5}, -2.4375×10^{-14}	0.115323, ± 0.826429
0.06	-0.08721, -1.78611×10^{-11}	-5.36193×10^{-5}, -2.4644×10^{-14}	0.123931, ± 0.822906
0.08	-0.08286, -1.54902×10^{-11}	-6.11994×10^{-5}, -2.4910×10^{-14}	0.132147, ± 0.819383

Table 4. The exact positions (x_0, y_0) of the seven noncollinear equilibrium points for varying oblateness of the smaller primary body for the binary Kruger 60 system when $\mu = 0.3937$, $q_1 = 0.99992$, $q_2 = 0.99996$, $A_1 = 0.03$, $A_3 = 0.01$, $M_b = 0.1$, $T = 0.01$, and $c_d = 46{,}393.84$

A_2	L_1	L_2	L_3
0	0.237373, -4.77803×10^{-11}	1.18483, -1.38057×10^{-9}	-1.12513, 3.30815×10^{-9}
0.02	0.224065, -4.71686×10^{-11}	1.19513, -1.35433×10^{-9}	-1.11921, 3.26603×10^{-9}
0.04	0.213770, -4.62386×10^{-11}	1.20382, -1.33011×10^{-9}	-1.11348, 3.22549×10^{-9}
0.06	0.205342, -4.52126×10^{-11}	1.21131, -1.30752×10^{-9}	-1.10792, 3.18644×10^{-9}
0.08	0.198198, -4.41736×10^{-11}	1.21788, -1.28632×10^{-9}	-1.10253, 3.14877×10^{-9}
A_2	L_{n1}	L_{n2}	$L_{4(5)}$
0	-0.09570, -2.29841×10^{-11}	-4.31260×10^{-5}, -2.3966×10^{-14}	0.120363, ± 0.831079
0.02	-0.09584, -2.33171×10^{-11}	-4.22518×10^{-5}, -2.4239×10^{-14}	0.110861, ± 0.828187
0.04	-0.09598, -2.36487×10^{-11}	-4.13776×10^{-5}, -2.4509×10^{-14}	0.101827, ± 0.825231

0.06	$-0.09612, -2.39790\times 10^{-11}$	$-4.05034\times 10^{-5}, -2.4776\times 10^{-14}$	$0.093220, \pm 0.822227$
0.08	$-0.09625, -2.43080\times 10^{-11}$	$-3.96292\times 10^{-5}, -2.5041\times 10^{-14}$	$0.085005, \pm 0.819191$

Table 5. The exact positions (x_0, y_0) of the seven noncollinear equilibrium points for varying oblate infinitesimal body for the binary Kruger 60 system when $\mu = 0.3937$, $q_1 = 0.99992$, $q_2 = 0.99996$, $A_1 = 0.03$, $A_2 = 0.02$, $M_b = 0.1$, $T = 0.01$, and $c_d = 46{,}393.84$

A_3	L_1	L_2	L_3
0	$0.228817, -4.83841\times 10^{-11}$	$1.18723, -1.35292\times 10^{-9}$	$-1.11302, 3.27131\times 10^{-9}$
0.02	$0.219938, -4.59976\times 10^{-11}$	$1.20251, -1.35576\times 10^{-9}$	$-1.12512, 3.26119\times 10^{-9}$
0.04	$0.213051, -4.38161\times 10^{-11}$	$1.21599, -1.35862\times 10^{-9}$	$-1.13624, 3.25260\times 10^{-9}$
0.06	$0.207463, -4.18494\times 10^{-11}$	$1.22812, -1.36146\times 10^{-9}$	$-1.14654, 3.24522\times 10^{-9}$
0.08	$0.202793, -4.00781\times 10^{-11}$	$1.23917, -1.36425\times 10^{-9}$	$-1.15615, 3.23880\times 10^{-9}$
A_3	L_{n1}	L_{n2}	$L_{4(5)}$
0	$-0.09953, -2.61418\times 10^{-11}$	$-3.8900\times 10^{-5}, -2.42387\times 10^{-14}$	$0.110973, \pm 0.823487$
0.02	$-0.09266, -2.10557\times 10^{-11}$	$-4.5604\times 10^{-5}, -2.42390\times 10^{-14}$	$0.110756, \pm 0.832774$
0.04	$-0.08740, -1.76425\times 10^{-11}$	$-5.2308\times 10^{-5}, -2.42394\times 10^{-14}$	$0.110564, \pm 0.841631$
0.06	$-0.08314, -1.51760\times 10^{-11}$	$-5.9015\times 10^{-5}, -2.42397\times 10^{-14}$	$0.110393, \pm 0.850101$
0.08	$-0.07958, -1.33034\times 10^{-11}$	$-6.5723\times 10^{-5}, -2.42401\times 10^{-14}$	$0.110239, \pm 0.858221$

Next, since we have computed the coordinates (x_0, y_0) of the equilibrium points (presented in Tables 2—5), we can insert them into the characteristic equation (8) and thus derive their linear stability numerically. In Table 6, we show the eigenvalues of the equilibrium points under the combined effect of oblateness, circumbinary disc, radiation pressure and P-R drag for the binary system. In this case, our numerical exploration in the computation of these roots as shown in Table 6 reveals that all the equilibria are unstable due to a positive real roots or a complex root with positive real part except for the equilibrium point L_{n2} where we get complex roots with negative real parts, which means that this point is stable.

Table 6: The exact positions (x_0, y_0) and eigenvalues of the seven non-collinear equilibrium points in the vicinity of Kruger 60 binary system when $\mu = 0.3937$, $q_1 = 0.99992$, $A_1 = 0.024$, $A_2 = 0.02$, $A_3 = 0.015$, $M_b = 0.06$, $T = 0.01$, and $c_d = 46{,}393.84$

L_i	(x_0, y_0)	$\lambda_{1,2}$	$\lambda_{3,4}$
L_1	$(0.202605, -5.86602\times 10^{-11})$	± 6.27847	$-2.78734\times 10^{-9} \pm 4.32354i$
L_2	$(1.216090, -1.41973\times 10^{-9})$	± 1.57883	$-1.51791\times 10^{-9} \pm 1.50988i$
L_3	$(-1.13709, 3.37511\times 10^{-9})$	± 1.20201	$-2.89857\times 10^{-9} \pm 1.35229i$
L_{n1}	$(-0.08054, -2.18648\times 10^{-11})$	± 17.5167	$-5.77124\times 10^{-9} \pm 12.0606i$
L_{n2}	$(-6.94460, -3.86392\times 10^{-14})$	$-5.83979\times 10^{-9} \pm 243.799i$	$-5.66617\times 10^{-9} \pm 246.015i$
$L_{4(5)}$	$(0.108112, \pm 0.842258)$	$-5.83979\times 10^{-9} \pm 243.799i$	$0.718745 \pm 1.03258i$

RESULTS AND DISCUSSION

The existence, position and stability of the equilibrium points in the photogravitational restricted three-body problem (R3BP) that accounts for Poynting-Robertson (P-R) drag, circumbinary disc with three oblate bodies were studied. The equations of motion of the present study and those described by Singh and Amuda (2017) differ due to the oblate infinitesimal body and potential from the belt in the present study. In accordance with previous studies, the emergence of new equilibria also takes place in the perturbed circular restricted problem of three bodies with circumbinary disc. We found that five or seven equilibrium points may lie on the plane of motion of the primaries. Moreover, it was observed that the existence and positions of these points are affected by the model's parameters. This comes directly by the pertinent non-linear algebraic equations, which provide the respective locations, since it was observed that in the presence of P-R drag effect the well-known collinear equilibrium points of the circular restricted three-body problem cease to exist both analytically and numerically in contrast to the absence of the aforementioned perturbing force, i.e., the P-R drag effect, where the collinear equilibria always exist and the distribution of equilibria on the plane of motion differs as a result of the disc and mass parameter. Additionally, it was observed that the involved parameters of the problem not only affect the number and positions of the corresponding equilibria but also influence their stability as well since it was identified that there are values of these parameters for which the points may be linearly stable.

Finally, a numerical exploration, using the binary system Kruger 60, was performed to locate the positions of equilibrium points of the system as well as their linear stability. These points were shown numerically and graphically, thus highlighting the effects of the involved parameters. For the determination of the stability of the infinitesimal body's motion around the obtained equilibrium points, we linearized the governing equations of motion around them. For the stability of the seven equilibria, the four roots of the characteristic polynomial were determined numerically and found that all points of equilibrium are always linearly unstable, except equilibrium point L_{n2}, which is linearly stable (Table 6). Also, contrary to the classical restricted three-body where the three collinear points are generally unstable and the triangular points are linearly stable for sufficiently small ratio of the two masses (see e.g., Szebehenly, 1967) or the restricted three-body problem under the effect of radiation and angular velocity variation of the two primary bodies where these five equilibria may be stable (see Perdios et al. 2015), we observed that for the problem under investigation all the five equilibria are unstable due to the presence of the P-R drag effect. However, the inclusion of the P–R effect cannot alter the stability state of L_{n2} in the case of seven EPs as it remains stable.

CONCLUSION

By taking perturbations in the radiation pressure, Poynting-Robertson drag and circumbinary disc with oblateness of the primaries together with an oblate infinitesimal mass body, the existence, positions of equilibrium points and their linear stability have been established. It is observed that the number and positions of the equilibrium points are affected by the model's parameters. It is further seen that in spite of the introduction of aforementioned parameters the equilibrium point L_{n2}remain stable.

FUNDING STATEMENT

During this work the first author, U. M. Udo was in receipt of "Tertiary Education Trust Fund (tetfund)- Nigeria" 2021 Institution-Based Research Grant.

REFERENCES

Abouelmagd, E. I , Asiri, H. M. and Sharaf , M. A., (2013). Effect of oblateness in the perturbed restricted three-body problem," *Meccanica*. 48, 2479–2490.

Capdevila, L.R and Howell, K.C. (2018). A transfer network linking Earth, Moon, and the triangular libration point regions in the Earth-Moon system. *Adv. Space. Res*. 62, 1826–1852.

Chernikov, J. A. (1970). The photogravitational restricted three-body problem. *Sov. Astron*. 14, 176–181.

Gao, F. and Wang, R. (2020). Bifurcation analysis and periodic solutions of the HD 191408 system with triaxial and radiative perturbations. *Universe* **6**, 35.

Gyegwe, J. M., Vincent, A. E. and Perdiou, A.E. (2022). On the stability of the triangular equilibrium points in the photogravitational R3BP with an oblate infinitesimal and triaxial primaries for the binary Lalande 21258 system, in Approximation and Computation in Science and Engineering, ed. by Th. M. Rassias and P. Pardalos. Springer Optim. Its Appl. 180 (Springer, Cham,) 397—415.

Jiang, I. G. and Yeh, L. C. (2004). The drag-induced resonant capture for Kuiper Belt objects. *Mon. Not. R. Astron. Soc*. 355, 29–32.

Jiang, I. G. and Yeh, L. C. (2006). On the Chermnykh-like problem: The equilibrium points, *Astrophys. Space Sci*. 305, 341–345.

Kalantonis, V. S., Perdios, E. A. and Perdiou, A. E. (2008). The Sitnikov family and the associated families of 3D periodic orbits in the photogravitational RTBP with oblateness. *Astrophys. Space Sci.* 315, 323–334.

Kalantonis, V. S., Vincent, A. E., Gyegwe, J. M., and Perdios, E. A. (2021). "Periodic Solutions Around the Out-Of-Plane Equilibrium Points in the Restricted Three-Body Problem with Radiation and Angular Velocity Variation" in Nonlinear Analysis and Global Optimization. Editors Th. M. Rassias and P. M. Pardalos (Cham: Springer), 251–275. Springer Optimization and Its Applications. doi:10.1007/978-3-030-61732-5_11

Kishor, R. and Kushvah, B. S. (2013). Linear stability and resonances in the generalized photogravitational Chermnykh-like problem with a disc. *Mon. Not. R. Astron. Soc.* 436, 1741–1749.

Leke,O. and Singh, J. (2021). Exploring Effect of Perturbing Forces on Periodic Orbits in the Restricted Problem of Three Oblate Spheroids with Cluster of Material Points. *Int. Astron. and Astrophy. Research J.,* 2(4), 48-73.

Lhotka , C. and Celletti, A. (2015).The effect of Poynting-Robertson drag on the triangular Lagrangian points. *Icarus*. 250, 249–261

Orbeti, P. and Vienne, A. (2003). An upgrade theory for Helene Telesto, and Calypso. *Astron. Astrophy*. 397: 353—359.

Papadakis, K.E. (1996). Families of periodic orbits in the photogravitational three-body problem, AP&SS, 245, 1—13

Papadakis, K.E. (1995). The geometry of the Roche coordinates and zero-velocity curves in the photogravitational three-body problem, *Astrophys. Space Sci.* 232, 337–354

Papadakis, K.E. (2006). The planar photogravitational Hill problem. Int. J. Bifurcat. Chaos, 16, 1809–1821

Papadakis, K., Ragos, O., and Litzerinos C. (2009). Asymmetric periodic orbits in the photogravitational Copenhagen problem. Journal of Computational and Applied Mathematics 227, 102-114

Pal, A. K. and Kushvah, B.S. (2015). Geometry of halo and Lissajous orbits in the circular restricted three-body problem with drag forces. *Mon Not R Astron Soc*..46(1), 959–72.

Perdios, E.A., Kalantonis, V.S., Perdiou, A.E., Nikaki, A.A., (2015). Equilibrium points and related periodic motions in the restricted three- body problem with angular velocity and radiation effects. Adv. Astron. 2015, 473–483.

Poynting, J. H. (1903). Radiation in the solar system: its effect on temperature and its pressure on small bodies. Philos. Trans. Roy. Soc. London 202, 525–552.

Radzievskii , V.V. (1950). The restricted problem of three bodies taking account of light pressure. *Astron. Zh*. 27, 250–256.

Radzievskii, V.V. (1953). The space photogravitational restricted three-body problem. *Astron. Zh*.. 30, 25–273.

Ragos, O. and Zafiropoulos, F. A. (1995). A numerical study of the influence of the Poynting-Robertson effect on the equilibrium points of the photogravitational restricted three–body problem. I. Coplanar case. *Astron. Astrophys*. 300, 568–578.

Robertson, H. P. (1937). Dynamical effects of radiation in the solar system. *MNRAS*. 97, 423–438,.

Schuerman, D.W. (1980). The restricted three-body problem including radiation pressure. *Astrophys. J.* **238**, 337–342

Simmons, J. F. L, McDonald, A. J. C. and Brown, J. C. (1985). The restricted 3–body problem with radiation pressure. *Celest. Mech*. 35, 145–187.

Singh, J. and Amuda, T. O. (2017). Effects of Poynting-Robertson (P-R) drag, radiation, and oblateness on motion around the L4,5 equilibrium points in the CR3BP. *J. Dyn. Syst. Geom. Theor*. 15, 177.

Singh, J. and Taura, J. J. (2013). Motion in the generalized restricted three-body problem. *Astrophys. Space Sci.* 343, 95–106.

Stenborg ,T. N. (2008). Collinear Lagrange point solutions in the circular restricted three-body problem with radiation pressure using Fortran. In: Argyle, R.W., Bunclark, P.S., Lewis, J.R. (Eds.), Astronomical Data Analysis Software and Systems XVII, *Astronomical Society of the Pacific Conference Series*. 394,734–737.

Stanley, P. and Whipple, F. L. (1950). The Poynting-Robertson effects on meteor orbits. *Am Astron Soc*. 111,134–141

Szebehely, V.G., 1967. Theory of Orbits. Academic Press, New York.

Taura and Leke (2022). Derivation of the dynamical equations of motion of the R3BP with variable masses and disk. *FUDMA Journal of Sciences (FJS*) 6 (4): 125 – 133.

Tyokyaa, K. R. and Atsue, T (2020). Positions and stability of libration points in the radiating and oblating bigger primary of circular restricted three-body problem. *FUDMA Journal of Sciences (FJS*) 4 (2) :523 – 531

Vincent, A. E. and Perdiou, A. E. (2021a). Poynting-Robertson and oblateness effects on the equilibrium points of the perturbed R3BP: Application on Cen X-4 binary system, in eds. T. M. Rassias, *Nonlinear Analysis, Differential Equations, and Applications, Springer Optim. Its App*. 173, 131–147.

Vincent, A. E. and Kalantonis, V.S. (2023). Motion around the equilibrium points in the photogravitational R3BP under the effects of Poynting-Robertson drag, circumbinary belt and triaxial primaries with an oblate infinitesimal body: Application on Achird Binary System, in Th. M. Rassias and P. Pardalos, (Eds) Analysis, Geometry, Nonlinear Optimization and Applications, Springer, Cham. https://doi.org/10.1142/9789811261572

Vincent, A. E. and Singh, J. (2022). Out-of-plane equilibria in the perturbed photogravitational restricted three-body problem with Poynting-Robertson drag, Heliyon, 8, e09603 doi.org/10.1016/j.heliyon.2022. e09603.

Vincent, A. E., Perdiou A. E. and Perdios, E.A. (2022). Existence and stability of equilibrium points in the R3BP with triaxial-radiating primaries and an oblate massless body under the effect of the circumbinary disc. *Fron. Astron. Space Sci*. 9:877459

Vincent, A. E. and Perdiou, A. E. (2021b). Existence and stability of equilibrium points under the influence of Poynting-Robertson and Stokes drags in the restricted three-body problem", in Rassias Th.M., Parasidis, I. N., Providas, E. (Eds) *Mathematical Analysis in Interdisciplinary Research*, Springer, Cham. DOI: 10.1007/978-3-030-84721-0-37

Vincent, A. E., Tsirogiannis, G. A., Perdiou, A. E., and Kalantonis, V. S. (2024). Equilibrium Points and Lyapunov Families in the Circular Restricted Three-body Problem with an Oblate Primary and a Synchronous Rotating Dipole Secondary: Application to Luhman-16 Binary System. New Astronomy 105 (2024) 102108

Vincent, A. E., Taura, J. J. and Omale, S. O. (2019): Existence and stability of equilibrium points in the photogravitational restricted four- body problem with Stokes drag effect, Astrophysics and Space Science 364 (10)

Yousuf, S. and Kishor, R. (2019). Effects of the albedo and disc on the zero velocity curves and linear stability of equilibrium points in the generalized restricted three-body problem. *Monthly Notices of the Royal Astronomical Society*. 488(2), 1894–1907.